

GSI-Preprint-2003-17

On baryon resonances and chiral symmetry

E.E. Kolomeitsev^a and M.F.M. Lutz^{b,c}

^a*The Niels Bohr Institute
Blegdamsvej 17, DK-2100 Copenhagen
Denmark*

^b*Gesellschaft für Schwerionenforschung (GSI),
Planck Str. 1, 64291 Darmstadt, Germany*

^c*Institut für Kernphysik, TU Darmstadt
D-64289 Darmstadt, Germany*

Abstract

We study $J^P = (\frac{3}{2})^-$ baryon resonances as generated by chiral coupled-channel dynamics in the χ -BS(3) approach. Parameter-free results are obtained in terms of the Weinberg-Tomozawa term predicting the leading s-wave interaction strength of Goldstone bosons with baryon-decuplet states. In the 'heavy' SU(3) limit with $m_\pi = m_K \sim 500$ MeV the resonances turn into bound states forming a decuplet and octet representation of the SU(3) group. Using physical masses the mass splitting are remarkably close to the empirical pattern.

1 Introduction

In this letter we further test the conjecture [1,2,3,4,5,6,7,8,9] that baryon resonances not belonging to the large- N_c ground states may be generated dynamically by coupled-channel dynamics. In recent works [6,7,10,11] it was shown that chiral dynamics as implemented by the χ -BS(3) approach [6,7,9] provides a parameter-free prediction for the existence of a wealth of s-wave baryon resonances. The latter may be classified in the 'heavy' SU(3) limit as forming two mass-degenerate octet and one singlet states [1,2,3,4,5,11,12]. Related works that adhere to a different strategy not insisting on improved crossing-transformation properties of the scattering amplitudes are [13,14,15,16,12]. All these findings support our conjecture. In the SU(6) quark-model approach such s-wave resonances belong to a 70-plet, that contains many more resonance states [17]. An interesting question arises: what is the role played by the d-wave resonances belonging to the very same 70-plet as the s-wave resonances studied in [11]. The phenomenological model [8] generated successfully also

non-strange d-wave resonances belonging to the 70-plet by coupled-channel dynamics describing a large body of pion and photon scattering data.

Naively one may expect that chiral dynamics does not make firm predictions for d-wave resonances since the meson-baryon interaction in the relevant channels probes a set of counter terms presently unknown. However, this is not necessarily so. Since a d-wave baryon resonance couples to s-wave meson baryon-decuplet states chiral symmetry is quite predictive for such resonances under the assumption that the latter channels are dominant. This is in full analogy to the analysis of the s-wave resonances [1,2,3,4,5,10,11,12] that neglects the effect of the contribution of d-wave meson baryon-decuplet states. The empirical observation that the d-wave resonances $N(1520)$, $N(1700)$ and $\Delta(1700)$ have large branching fractions ($> 50\%$) into the inelastic $N\pi\pi$ channel, even though the elastic πN channel is favored by phase space, supports our assumption. A parameter-free scheme arises since the Weinberg-Tomozawa theorem predicts the leading s-wave interaction strength of Goldstone bosons not only with baryon-octet but also with baryon-decuplet states.

In this letter we explore whether the Weinberg-Tomozawa interaction of the meson baryon-decuplet sector has the potential to dynamically generate d-wave baryon resonances. We find that the chiral dynamics predicts the existence of octet and decuplet bound states in the 'heavy' $SU(3)$ limit. Those bound states disappear once the current quark masses of QCD are sufficiently small. It should be possible to test this prediction within lattice QCD [18]. Using physical current quark masses the predicted mass spectrum is remarkably consistent with the empirical spectrum. This finding complements a corresponding result [1,2,3,4,5,11,12] obtained for the s-wave baryon resonances for which chiral dynamics predicts 2 degenerate octet and one singlet state that also disappear for sufficiently small current quark masses.

2 Chiral coupled-channel dynamics: the χ -BS(3) approach

The starting point is the chiral $SU(3)$ Lagrangian (see e.g.[19]). The relevant term that encodes the prediction of Weinberg and Tomozawa [20] for the s-wave scattering lengths of Goldstone bosons with baryon-decuplet states is readily identified,

$$\mathcal{L}_{WT} = \frac{3i}{8f^2} \text{tr} \left((\bar{B}_\nu \gamma^\mu B^\nu) \cdot [\Phi, (\partial_\mu \Phi)]_- \right), \quad (1)$$

where we dropped terms that do not contribute to the on-shell scattering process at tree level. The $SU(3)$ meson and baryon fields are written in terms of their isospin symmetric components,

$$\begin{aligned}
\Phi &= \tau \cdot \pi + \alpha^\dagger \cdot K + K^\dagger \cdot \alpha + \eta \lambda_8 , \\
\bar{B} \cdot B &= \frac{1}{6} (\bar{\Delta} \mathcal{G} \Delta) \cdot \tau + \frac{1}{6} \bar{\Delta} \cdot \Delta (2 + \sqrt{3} \lambda_8) + \frac{1}{3} \bar{\Sigma} \cdot \Sigma - \frac{i}{3} \tau \cdot (\bar{\Sigma} \times \Sigma) \\
&+ \frac{1}{6} \bar{\Xi} \cdot \Xi (2 - \sqrt{3} \lambda_8) + \frac{1}{6} (\bar{\Xi} \sigma \Xi) \tau + \frac{1}{3} \bar{\Omega}^- \cdot \Omega^- (1 - \sqrt{3} \lambda_8) \\
&+ \frac{1}{\sqrt{6}} \bar{\Delta} (\Sigma \cdot T) \alpha + \frac{1}{\sqrt{6}} \alpha^\dagger (\bar{\Sigma} \cdot T^\dagger) \Delta - \frac{1}{3} \bar{\Sigma} (\Xi^t i \sigma_2 \sigma \alpha) \\
&+ \frac{1}{3} (\alpha^\dagger \sigma i \sigma_2 \bar{\Xi}^t) \Sigma + \frac{1}{\sqrt{6}} \bar{\Omega}^- (\alpha^\dagger \cdot \Xi) + \frac{1}{\sqrt{6}} (\bar{\Xi} \cdot \alpha) \Omega^- , \quad (2)
\end{aligned}$$

with the Gell-Mann matrices, λ_i , and the isospin doublet fields $K = (K^+, K^0)^t$ and $\Xi = (\Xi^0, \Xi^-)^t$. The isospin Pauli matrices $\sigma = (\sigma_1, \sigma_2, \sigma_3)$ act exclusively in the space of isospin doublet fields (K, N, Ξ) and the matrix valued isospin doublet α ,

$$\begin{aligned}
\alpha^\dagger &= \frac{1}{\sqrt{2}} (\lambda_4 + i \lambda_5, \lambda_6 + i \lambda_7) , \quad \tau = (\lambda_1, \lambda_2, \lambda_3) , \\
\mathcal{G}_i &= 3 \vec{T} \sigma_i \vec{T}^\dagger , \quad \vec{T} \cdot \vec{T}^\dagger = 1 , \quad T_i^\dagger T_j = \delta_{ij} - \frac{1}{3} \sigma_i \sigma_j . \quad (3)
\end{aligned}$$

The 4×2 matrices T_j in (3) describe the transition from isospin- $\frac{1}{2}$ to isospin- $\frac{3}{2}$ states. The scattering process is described by the amplitudes that follow as solutions of the coupled-channel Bethe-Salpeter equation,

$$\begin{aligned}
T_{\mu\nu}(\bar{k}, k; w) &= K_{\mu\nu}(\bar{k}, k; w) + \int \frac{d^4 l}{(2\pi)^4} K_{\mu\alpha}(\bar{k}, l; w) G_{\alpha\beta}(l; w) T_{\beta\nu}(l, k; w) , \\
G_{\mu\nu}(l; w) &= -i D(\frac{1}{2} w - l) S_{\mu\nu}(\frac{1}{2} w + l) , \quad (4)
\end{aligned}$$

where we suppress the coupled-channel structure for simplicity. The meson and decuplet propagators, $D(q)$ and $S_{\mu\nu}(p)$, are used in the notation of [8]. The scattering amplitude $T_{\mu\nu}(\bar{k}, k; w)$ decouples into various sectors characterized by isospin (I) and strangeness (S) quantum numbers. This decomposition follows from a corresponding one (see [8]) of the interaction Lagrangian,

$$\mathcal{L}_{WT}(\bar{k}, k; w) = \sum_{I,S} R_\mu^{(I,S)\dagger}(\bar{q}, \bar{p}) \gamma_0 g^{\mu\alpha} K_{\alpha\beta}^{(I,S)}(\bar{k}, k; w) g^{\beta\nu} R_\nu^{(I,S)}(q, p) , \quad (5)$$

where the column $R^{(I,S)}(q, p)$ specifies our phase convention for the isospin states. We introduced convenient kinematics:

$$w = p + q = \bar{p} + \bar{q} , \quad k = \frac{1}{2} (p - q) , \quad \bar{k} = \frac{1}{2} (\bar{p} - \bar{q}) , \quad (6)$$

where q, p, \bar{q}, \bar{p} are the initial and final meson and baryon 4-momenta. In Tab. 1 we collect $R^{(I,S)}(q, p)$ for all isospin and strangeness channels considered in

this work. Following the χ -BS(3) approach developed in [7,8] the interaction kernel is decomposed into a set of covariant projectors that have well defined total angular momentum (J), and parity (P),

$$\begin{aligned}
K_{\mu\nu}(\bar{k}, k; w) &= \sum_{J,P} K^{(J,P)}(\sqrt{s}) \mathcal{Y}_{\mu\nu}^{(J,P)}(\bar{q}, q, w), \\
\mathcal{Y}_{\mu\nu}^{(1/2,\pm)}(\bar{q}, q; w) &= \frac{1}{6} \left(\gamma_\mu - \frac{w_\mu}{w^2} \psi \right) \left(\mp 1 - \frac{\psi}{\sqrt{w^2}} \right) \left(\gamma_\nu - \frac{w_\nu}{w^2} \psi \right) . \\
\mathcal{Y}_{\mu\nu}^{(3/2,\pm)}(\bar{q}, q; w) &= \frac{1}{2} \left(g_{\mu\nu} - \frac{w_\mu w_\nu}{w^2} \right) \left(\mp 1 + \frac{\psi}{\sqrt{w^2}} \right) \\
&\quad - \frac{1}{6} \left(\gamma_\mu - \frac{w_\mu}{w^2} \psi \right) \left(\mp 1 - \frac{\psi}{\sqrt{w^2}} \right) \left(\gamma_\nu - \frac{w_\nu}{w^2} \psi \right) . \tag{7}
\end{aligned}$$

where we provide the projector, $\mathcal{Y}_{\mu\nu}^{(1/2,\pm)}(\bar{q}, q; w)$ describing p- and d-wave scattering with $J = 1/2$ and $\mathcal{Y}_{\mu\nu}^{(3/2,\pm)}(\bar{q}, q; w)$ relevant for s-and p-wave scattering with $J = 3/2$. The merit of the projectors is that they decouple the Bethe-Salpeter equation (4) into orthogonal sectors labelled by the total angular momentum J . Here we suppress an additional matrix structure that follows since for given parity and total angular momentum, $J \geq 3/2$, two distinct angular momentum states couple. In general, for given J , the projector form a 2×2 matrix, for which we displayed in (7) only its leading 11-component. The effect of the remaining components is phase-space suppressed and not considered here. Referring to the detailed discussion given in [7] we assume a systematic on-shell reduction of an effective interaction kernel,

$$V = K + \mathcal{O}(Q^3),$$

which is expanded according to chiral power counting rules. In addition, we insist on the renormalization condition,

$$T_{\mu\nu}^{(I,S)}(\bar{k}, k; w) \Big|_{\sqrt{s}=\mu(I,S)} = V_{\mu\nu}^{(I,S)}(\bar{k}, k; w) \Big|_{\sqrt{s}=\mu(I,S)}, \tag{8}$$

that complies with approximate crossing symmetry. For the subtraction points, $\mu(I, S)$, the natural choices are determined by the baryon-octet masses,

$$\begin{aligned}
\mu(I, +1) &= \mu(I, -3) = \frac{1}{2} (m_\Lambda + m_\Sigma), & \mu(I, 0) &= m_N, \\
\mu(0, -1) &= m_\Lambda, & \mu(1, -1) &= m_\Sigma, & \mu(I, -2) &= \mu(I, -4) = m_\Xi \tag{9}
\end{aligned}$$

as explained in detail in [7]. The renormalization condition reflects the fact that at subthreshold energies the scattering amplitudes may be evaluated in standard chiral perturbation theory with the typical expansion parameter $m_K/(4\pi f) < 1$ with $f \simeq 90$ MeV. Once the available energy is sufficiently

$(\frac{1}{2}, -4)$	$(0, -3)$	$(1, -3)$	$(\frac{1}{2}, -2)$		
$(\bar{K} \Omega^\mu)$	$\begin{pmatrix} (\frac{1}{\sqrt{2}} \bar{K} \Xi^\mu) \\ (\eta \Omega^\mu) \end{pmatrix}$	$\begin{pmatrix} (\pi \Omega^\mu) \\ (\frac{1}{\sqrt{2}} \bar{K} \sigma \Xi^\mu) \end{pmatrix}$	$\begin{pmatrix} (\frac{1}{\sqrt{3}} \pi \cdot \sigma \Xi^\mu) \\ (\frac{i}{\sqrt{3}} \Sigma^\mu \cdot \sigma \sigma_2 \bar{K}^t) \\ (\eta \Xi^\mu) \\ (K \Omega^\mu) \end{pmatrix}$		
$(\frac{3}{2}, -2)$	$(0, -1)$	$(1, -1)$	$(2, -1)$		
$\begin{pmatrix} (\pi \cdot T \Xi^\mu) \\ (\Sigma^\mu \cdot T i \sigma_2 \bar{K}^t) \end{pmatrix}$	$\begin{pmatrix} (\frac{1}{\sqrt{3}} \pi \cdot \Sigma^\mu) \\ (\frac{1}{\sqrt{2}} K^t i \sigma_2 \Xi^\mu) \end{pmatrix}$	$\begin{pmatrix} (\frac{-i}{\sqrt{2}} \pi \times \Sigma^\mu) \\ (\sqrt{\frac{3}{4}} \bar{K} \vec{T}^\dagger \Delta^\mu) \\ (\eta \Sigma^\mu) \\ (\frac{1}{\sqrt{2}} K^t i \sigma_2 \sigma \Xi^\mu) \end{pmatrix}$	$\begin{pmatrix} \frac{1}{2}(\pi_i \Sigma_j^\mu + \pi_j \Sigma_i^\mu) - \frac{1}{3} \delta_{ij} \pi \cdot \Sigma^\mu \\ \frac{1}{\sqrt{8}} \bar{K} (\sigma_i T_j^\dagger + \sigma_j T_i^\dagger) \Delta^\mu \end{pmatrix}$		
$(\frac{1}{2}, 0)$	$(\frac{3}{2}, 0)$	$(\frac{5}{2}, 0)$			
$\begin{pmatrix} (\frac{1}{\sqrt{2}} \pi \cdot T^\dagger \Delta^\mu) \\ (\frac{1}{\sqrt{3}} \Sigma^\mu \cdot \sigma K) \end{pmatrix}$	$\begin{pmatrix} (\frac{1}{\sqrt{15}} \pi \cdot \mathcal{G} \Delta^\mu) \\ (\eta \Delta^\mu) \\ (\Sigma^\mu T K) \end{pmatrix}$	$\left((\frac{1}{2} (\pi_i T_j^\dagger + \pi_j T_i^\dagger) - \frac{1}{3} \delta_{ij} \pi \cdot T^\dagger) \Delta^\mu \right)$			
$(1, 1)$	$(2, 1)$				
$(\sqrt{\frac{3}{4}} K^t i \sigma_2 \vec{T}^\dagger \Delta^\mu)$	$(\frac{1}{\sqrt{8}} K^t i \sigma_2 (\sigma_i T_j^\dagger + \sigma_j T_i^\dagger) \Delta^\mu)$				

Table 1

The column $R_\mu^{(I,S)}(q, p)$ for isospin (I) and strangeness (S).

high to permit elastic two-body scattering a further typical dimensionless parameter $m_K^2/(8\pi f^2) \sim 1$ arises. Since this ratio is uniquely linked to two-particle reducible diagrams it is sufficient to sum those diagrams keeping the perturbative expansion of all irreducible diagrams. This is achieved by (4). The subtraction points (9) are the unique choices that protect the s-channel baryon-octet masses manifestly in the p-wave $J = \frac{1}{2}$ scattering amplitudes. The merit of the scheme [10,6,7] lies in the property that for instance the $K \Xi$ and $\bar{K} \Xi$ scattering amplitudes match at $\sqrt{s} \sim m_\Xi$ approximately as expected from crossing symmetry. The subtraction points (9) can also be derived if one incorporates photon-baryon inelastic channels. Then additional crossing symmetry constraints arise. For instance the reaction $\gamma \Xi \rightarrow \gamma \Xi$, which is subject to a crossing symmetry constraint at threshold, may go via the intermediate states $\bar{K} \Lambda$ or $\bar{K} \Sigma$. Here we assume that this reaction is described by a coupled-channel scattering equation (4) where the effective on-shell interaction kernel V is expanded in chiral perturbation theory.

With the decomposition (7) the solution of the Bethe-Salpeter equation takes the form

(I, S)	11	12	22	13	23	33	14	24	34	44
$(\frac{1}{2}, -4)$	-3	-	-	-	-	-	-	-	-	-
$(0, -3)$	0	-3	0	-	-	-	-	-	-	-
$(1, -3)$	0	$-\sqrt{3}$	-2	-	-	-	-	-	-	-
$(\frac{1}{2}, -2)$	2	-1	2	0	-3	0	$\frac{3}{\sqrt{2}}$	0	$\frac{3}{\sqrt{2}}$	3
$(\frac{3}{2}, -2)$	-1	2	-1	-	-	-	-	-	-	-
$(0, -1)$	4	$\sqrt{6}$	3	-	-	-	-	-	-	-
$(1, -1)$	2	1	4	0	$-\sqrt{6}$	0	2	0	$-\sqrt{6}$	1
$(2, -1)$	-2	$\sqrt{3}$	0	-	-	-	-	-	-	-
$(\frac{1}{2}, 0)$	5	-2	2	-	-	-	-	-	-	-
$(\frac{3}{2}, 0)$	2	0	0	$\sqrt{\frac{5}{2}}$	$\frac{3}{\sqrt{2}}$	-1	-	-	-	-
$(\frac{5}{2}, 0)$	-3	-	-	-	-	-	-	-	-	-
$(1, 1)$	1	-	-	-	-	-	-	-	-	-
$(2, 1)$	-3	-	-	-	-	-	-	-	-	-

Table 2

The coefficient matrices $C^{(I,S)}$ of the Weinberg-Tomozawa term that characterize the meson baryon-decuplet interaction introduced in (13). The matrix elements are ordered according to the states in Tab. 1.

$$T_{\mu\nu}(\bar{k}, k; w) = \sum_{J,P} M^{(J,P)}(\sqrt{s}) \mathcal{Y}_{\mu\nu}^{(J,P)}(\bar{q}, q; w),$$

$$M^{(J,P)}(\sqrt{s}) = \left[1 - K^{(J,P)}(\sqrt{s}) J^{(J,P)}(\sqrt{s}) \right]^{-1} K^{(J,P)}(\sqrt{s}), \quad (10)$$

where the loop matrix $J_{ab}^{(J,P)}(\sqrt{s})$ is diagonal in the coupled-channel space. Diagonal elements are fully specified in terms of the meson and baryon-decuplet masses m and M entering the considered channel and a universal subtraction point $\mu = \mu(I, S)$ depending only on the isospin and strangeness quantum numbers. For the loop functions of the the different sectors with $J^P = (\frac{1}{2})^\pm, (\frac{3}{2})^\pm$ we find

$$J^{(J,P)}(\sqrt{s}) = N^{(J,P)}(\sqrt{s}) (I(\sqrt{s}) - I(\mu)),$$

$$I(\sqrt{s}) = \frac{1}{16\pi^2} \left(\frac{p_{\text{cm}}}{\sqrt{s}} \left(\ln \left(1 - \frac{s - 2p_{\text{cm}}\sqrt{s}}{m^2 + M^2} \right) - \ln \left(1 - \frac{s + 2p_{\text{cm}}\sqrt{s}}{m^2 + M^2} \right) \right) \right. \\ \left. + \left(\frac{1}{2} \frac{m^2 + M^2}{m^2 - M^2} - \frac{m^2 - M^2}{2s} \right) \ln \left(\frac{m^2}{M^2} \right) + 1 \right) + I(0), \quad (11)$$

where $\sqrt{s} = \sqrt{M^2 + p_{\text{cm}}^2} + \sqrt{m^2 + p_{\text{cm}}^2}$ and $E = \sqrt{M^2 + p_{\text{cm}}^2}$ and

$$\begin{aligned}
N^{(1/2,\pm)}(\sqrt{s}) &= (E \mp M) \left(\frac{2}{9} \frac{E^2}{M^2} - \frac{2}{9} \right), \\
N^{(3/2,\pm)}(\sqrt{s}) &= (E \mp M) \left(\frac{5}{9} + \frac{2}{9} \frac{E}{M} + \frac{2}{9} \frac{E^2}{M^2} \right).
\end{aligned} \tag{12}$$

It is left to identify the interaction kernel $K_{ab}^{(J,P,I,S)}(\sqrt{s})$ as predicted by the Weinberg-Tomozawa term (1). The coupled-channel structure is made explicit, with a and b referring to initial and final states,

$$\begin{aligned}
K_{ab}^{(\frac{1}{2},\pm,I,S)}(\sqrt{s}) &= \frac{C_{ab}^{(I,S)}}{4 f^2} (2 \sqrt{s} \mp M_a \mp M_b), \\
K_{ab}^{(\frac{3}{2},\pm,I,S)}(\sqrt{s}) &= \frac{C_{ab}^{(I,S)}}{4 f^2} (2 \sqrt{s} \pm M_a \pm M_b),
\end{aligned} \tag{13}$$

and M_a and M_b denoting the isospin averaged decuplet masses of initial and final channel. The interaction kernels are identical for the two channels, $J = \frac{1}{2}$ and $J = \frac{3}{2}$, considered here. The ' \pm ' in (13) keeps track of the parity quantum number with $P = \pm 1$. The values for the coefficient matrix $C_{ab}^{(I,S)}$ characterizing the strength of the Weinberg-Tomozawa term in the coupled-channel space are collected in Tab. 2. A remark of caution is in order here. Though we provide here the contribution of the Weinberg-Tomozawa term to the leading channels, it should be emphasized that only for $J^P = (\frac{3}{2})^-$ the term constitutes the dominant contribution to the interaction kernel. In the remaining channels there exist further terms in the chiral Lagrangian, so far basically unknown, that may change the interaction kernel significantly. Nevertheless it is instructive to study the consequence of the Weinberg-Tomozawa term in those channels as it is. One may draw qualitative conclusion as to whether the chiral Lagrangian has the potential to dynamically generate $J^P = (\frac{3}{2})^+$ and $J^P = (\frac{1}{2})^\pm$ baryon resonances as well.

3 Results

In order to study the formation of baryon resonances we generate speed plots as suggested by Höhler [21]. The speed, $\text{Speed}_{ab}^{(J,P)}(\sqrt{s})$, of a given channel $a b$ is introduced by [21,22],

$$\begin{aligned}
t_{ab}^{(J,P)}(\sqrt{s}) &= \frac{1}{8 \pi \sqrt{s}} \left(p_{\text{cm}}^{(a)} N_a^{(J,P)}(\sqrt{s}) p_{\text{cm}}^{(b)} N_b^{(J,P)}(\sqrt{s}) \right)^{1/2} M_{ab}^{(J,P)}(\sqrt{s}), \\
\text{Speed}_{ab}^{(J,P)}(\sqrt{s}) &= \left| \sum_c \left[\frac{d}{d \sqrt{s}} t_{ac}^{(J,P)}(\sqrt{s}) \right] \left(\delta_{cb} + 2 i t_{cb}^{(J,P)}(\sqrt{s}) \right)^\dagger \right|.
\end{aligned} \tag{14}$$

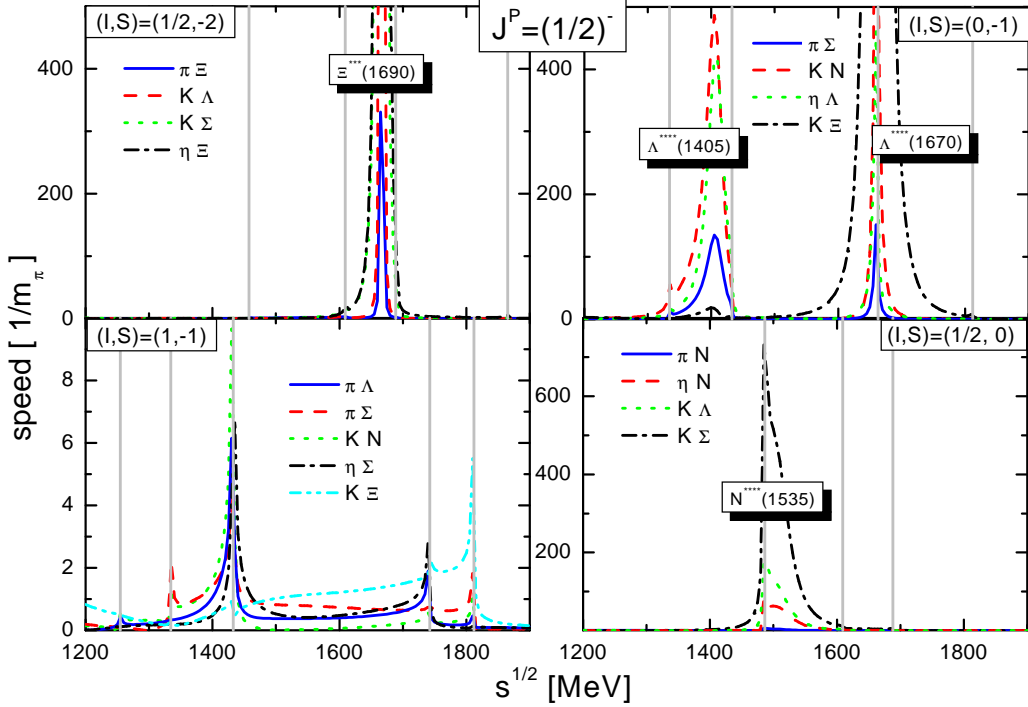


Fig. 1. Diagonal speed plots of the $J^P = (\frac{1}{2})^-$ sector. The vertical lines show the opening of inelastic meson baryon-decuplet channels. Parameter-free results are obtained in terms of physical masses and $f = 90$ MeV [11].

If a resonance with not too large decay width sits in the amplitude $M^{(J,P)}(\sqrt{s})$ a clear peak structure emerges in the speed plot even if the resonance structure is masked by a background phase.

We begin with a discussion of our results in the SU(3) limit. The latter is not defined uniquely depending on the magnitude of the current quark masses, $m_u = m_d = m_s$. We study this dependence at chiral order Q^2 . Using the meson-baryon sigma terms of [7] a meson mass $m_{[8]} \simeq m_K$ implies for instance a baryon-octet mass $M_{[8]} \simeq 1275$ MeV. Applying the large- N_c limit one may use $M_{[8]} = M_{[10]}$ for the baryon-decuplet masses. This scenario we call the 'heavy' SU(3) limit. Similarly we introduce the notion of a 'light' SU(3) limit with $m_{[8]} = m_\pi$ and $M_{[8]} \simeq 860$ MeV.

Before discussing our results for meson baryon-decuplet scattering we briefly recall the results of the recent work [11] which addressed the chiral dynamics of s-wave meson baryon-octet states. In the SU(3) limit meson baryon-octet scattering is classified according to,

$$8 \otimes 8 = 27 \oplus \overline{10} \oplus 10 \oplus 8 \oplus 8 \oplus 1. \quad (15)$$

The Weinberg and Tomozawa interaction predicts attraction in the two 8-plet

and the 1-plet channel but repulsion in the 27-plet channel [12]. The repulsion in the 27-plet channels follows for instance from the negative signs of the coefficients $C^{(I,S)}$ in the (1,1) and (2,-1) sectors that involve one channel only (see e.g. [7]). All together the 27-plet has contributions in nine channels with

$$(I, S)_{[27]} = (1, 1), (\frac{3}{2}, 0), (\frac{1}{2}, 0), (2, -1), (1, -1), (0, -1), (\frac{3}{2}, -2), (\frac{1}{2}, -2), (1, -3).$$

Similarly the $\overline{10}$ -plet and 10-plet contribute in

$$(I, S)_{\overline{10}} = (0, 1), (\frac{1}{2}, 0), (1, -1), (\frac{3}{2}, -2),$$

$$(I, S)_{10} = (\frac{3}{2}, 0), (1, -1), (\frac{3}{2}, -2), (0, -3).$$

The vanishing of $C^{(0,1)}$ (see e.g. [7]) tells that the interaction strength vanishes in the $\overline{10}$ -plet channel [12]. An analogous result [12] holds for the 10-plet channel. This follows most efficiently from the vanishing of $C^{(0,-3)}$. As a consequence in the 'heavy' SU(3) limit the chiral dynamics predicts two degenerate octet bound states together with a non-degenerate singlet state [1,2,3,4,5,11,12]. In the 'light' SU(3) limit all states disappear leaving no clear signal in any of the speed plots. Using physical meson and baryon-octet masses the bound-state turn into resonances as shown in Fig. 1. The speed plots show strong evidence for the formation of the $\Xi(1690)$, $\Lambda(1405)$, $\Lambda(1670)$ and $N(1535)$ resonances. The 'disappearance' of the remaining states was discussed in detail in [11].

We turn to the meson baryon-decuplet scattering process, — the focus of this work. In the SU(3) limit this process decouples into four different channels, labelled according to,

$$8 \otimes 10 = 35 \oplus 27 \oplus 10 \oplus 8. \quad (16)$$

In the $J^P = \frac{3}{2}^-$ sector the Weinberg-Tomozawa interaction is attractive in the 8-plet, 10-plet and 27-plet channel, but repulsive in the 35-plet channel. Therefore one may expect resonances or bound states in the former channels. For instance, the repulsion in the 35-plet channel with

$$(I, S)_{35} = (2, 1), (\frac{5}{2}, 0), (\frac{3}{2}, 0), (2, -1), (1, -1), (\frac{3}{2}, -2), (\frac{1}{2}, -2), (1, -3), (0, -3), (\frac{1}{2}, -4), \quad (17)$$

follows from the negative $C^{(I,S)}$ coefficients (see Tab. 2) in the (2,1) and $(\frac{1}{2}, -4)$ sectors. Similarly the positive $C^{(1,1)}$ coefficients reflects the weak attraction in the 27-plet channel. Indeed, in the 'heavy' SU(3) limit we find $72 = 4 \times (8 + 10)$ bound states of masses 1620 MeV and 1710 MeV forming an octet and decuplet representation of the SU(3) group. We do not find a 27-plet bound state reflecting the weaker attraction in this channel. However, if we

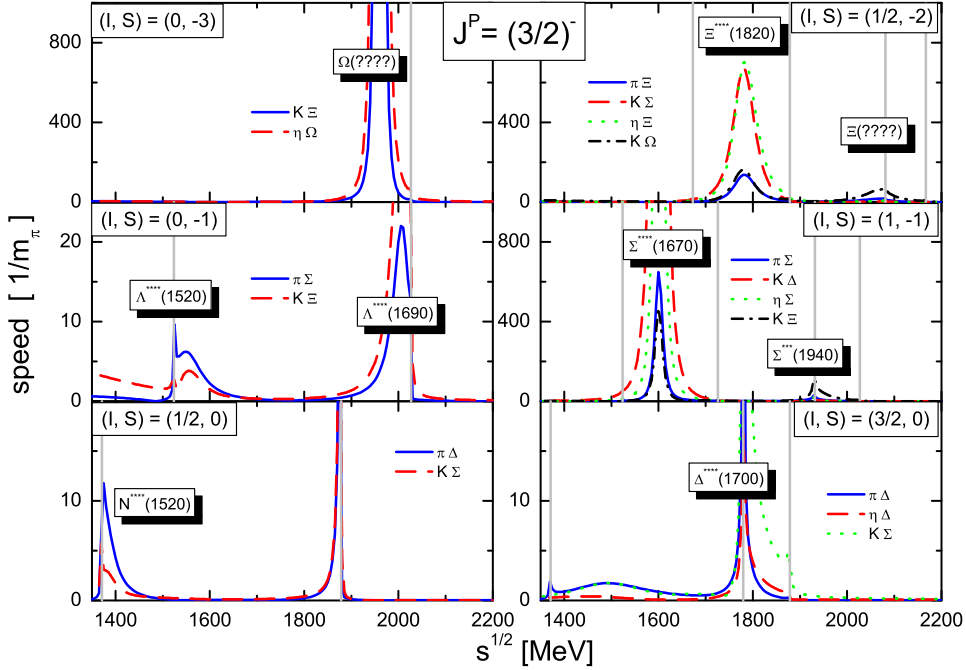


Fig. 2. Diagonal speed plots of the $J^P = (\frac{3}{2})^-$ sector. The vertical lines show the opening of inelastic meson baryon-decuplet channels. Parameter-free results are obtained in terms of physical masses and $f = 90$ MeV.

artificially increase the amount of attraction by about only 20 % by lowering the value of f a clear bound state arises in this channel. These phenomena persist if we use somewhat larger baryon-decuplet masses. A contrasted result is obtained if we lower the meson masses down to the pion mass arriving at the 'light' SU(3) limit. Then we find neither bound nor resonance octet or decuplet states. Increasing the baryon-decuplet mass somewhat away from the baryon-octet mass does not change this result.

Even though the Weinberg-Tomozawa term does not constitute the complete leading order interaction in the $J^P = (\frac{1}{2})^\pm$ and $J^P = (\frac{3}{2})^+$ channels it is nevertheless instructive to explore the consequences thereof in those sectors. Using physical masses we observe in the speed plots of the $J^P = (\frac{1}{2})^+$ sector octet and decuplet resonances with masses centering around 2000 MeV. Of course the resonances of this channel are dominated by s-wave meson baryon-octet channels [11] and one should not expect any realistic results in terms of d-wave meson baryon-decuplet channels only. Similarly we do not find any clear signal of $J^P = (\frac{1}{2})^-$ and $J^P = (\frac{3}{2})^+$ resonances in the p-wave channels of masses below 2000 MeV.

We turn to the central result of this work. In Fig. 2 speed plots of the $J^P = (\frac{3}{2})^-$ sector are shown for all channels in which octet and decuplet resonance

states are expected. It is a remarkable success of the present scheme that it predicts parameter free the four-star hyperon resonances $\Xi(1820)$, $\Lambda(1520)$, $\Sigma(1670)$ with masses quite close to the empirical values. The nucleon and isobar resonances $N(1520)$ and $\Delta(1700)$ also present in Fig. 1, are predicted with less accuracy. The important result here is the fact that those resonances are generated at all. It should not be expected to arrive already at fully realistic results in this leading order calculation. For instance chiral correction terms provide a d-wave π Δ -component of the $N(1520)$.

We continue with the peak in the (0,-3)-speeds at mass 1950 MeV. Since this is below all thresholds it is in fact a bound state. Such a state has so far not been observed but is associated with a decuplet resonance. It is a clear and solid prediction of our scheme and we suggest to search for such a state. Typically such a state is predicted to have resonance character in large- N_c phenomenology and quark-model calculations with a mass above 2000 MeV [17]. Further states belonging to the decuplet are seen in the $(\frac{1}{2}, -2)$ - and $(1, -1)$ -speeds at masses 2100 MeV and 1920 MeV. The latter state can be identified with the three star $\Xi(1940)$ resonance. Finally we point at the fact that the $(0, -1)$ -speeds show signals of two resonance states consistent with the existence of the four star resonance $\Lambda(1520)$ and $\Lambda(1690)$ even though in the 'heavy' SU(3) limit we observed only one bound state. It appears that the SU(3) symmetry breaking pattern generates the 'missing' 'singlet' state not predicted by (16).

It should be noted that the mass and widths parameters one may extract from the speed plots in Fig. 1 could be improved by incorporating contributions from meson baryon-octet decays not considered here. In particular one would expect from previous phenomenological studies like [8] that the vector-meson baryon-octet channels may play an important role in the course of improving the results of this work. One may speculate that the weak attraction found in the 27-plet channel which is almost strong enough to generate resonance structures could generate states with anomalous quantum numbers like $(I, S) = (1, 1)$ if the correction terms conspire to slightly increase the attraction found already at leading order.

Acknowledgments

The authors thank the ECT* for hospitality and pleasant working conditions. E.K. acknowledges partial support from GSI.

References

[1] H.W. Wyld, Phys. Rev. **155** (1967) 1649.

- [2] R.H. Dalitz, T.C. Wong and G. Rajasekaran, Phys. Rev. **153** (1967) 1617.
- [3] J.S. Ball and W.R. Frazer, Phys. Rev. Lett. **7** (1961) 204.
- [4] G. Rajasekaran, Phys. Rev. **5** (1972) 610.
- [5] R.K. Logan and H.W. Wyld, Phys. Rev. **158** (1967) 1467.
- [6] M.F.M. Lutz und E.E. Kolomeitsev, Found. Phys. **31** (2001) 1671.
- [7] M.F.M. Lutz and E. E. Kolomeitsev, Nucl. Phys. **A 700** (2002) 193.
- [8] M.F.M. Lutz, Gy. Wolf and B. Friman, Nucl. Phys. **A 706** (2002) 431.
- [9] M.F.M. Lutz, GSI-Habil-2002-1.
- [10] M.F.M. Lutz and E. E. Kolomeitsev, Proc. of Int. Workshop XXVIII on Gross Properties of Nuclei and Nuclear Excitations, Hirschegg, Austria, January 16-22, 2000.
- [11] C. García-Recio, M.F.M. Lutz and J. Nieves, GSI-Preprint-2003-16; nucl-th/0305100.
- [12] D. Jido, J. A. Oller, E. Oset, A. Ramos and U. G. Meissner, nucl-th/0303062.
- [13] J. Nieves and E. Ruiz Arriola, Phys. Rev. **D 63**, (2001) 076001.
- [14] C. García-Recio, J. Nieves, E. Ruiz Arriola and M. J. Vicente-Vacas, Phys. Rev. **D67** (2003) 076009.
- [15] A. Ramos, E. Oset and C. Bennhold, Phys. Rev. Lett. **89** (2002) 252001.
- [16] E. Oset, A. Ramos, C. Bennhold, Phys. Lett. **B 527** (2002) 99.
- [17] C.L. Schat, J.L. Goity and N.N. Scoccola, Phys. Rev. Lett. **88** (2002) 102002.
- [18] D. G. Richards, Proc. of 'NSTAR 2002', Pittsburgh, October 2002, and references therein.
- [19] A. Krause, Helv. Phys. Acta **63** (1990) 3.
- [20] S. Weinberg, Phys. Rev. Lett. **17** (1966) 616; Y. Tomozawa, Nuov. Cim. **A46** (1966) 707.
- [21] G. Höhler, πN NewsLetter **9** (1993) 1.
- [22] F.T. Smith, Phys. Rev. **118** (1960) 349.